Effect of metformin therapy on cardiac function and survival in a volume-overload model of heart failure in rats

Jan BENES[*][†][‡], **Ludmila KAZDOVA**[†], **Zdenek DRAHOTA**[§], **Josef HOUSTEK**[§],
Dasa MEDRIKOVA[§], **Jan KOPECKY**[§], **Nikola KOVAROVA**[§], **Marek VRBACKY**[§],
David SEDMERA[§][‖], **Hynek STRNAD**[¶], **Michal KOLAR**[¶], **Jiri PETRAK**[**][††],
Oldrich BENADA[‡‡], **Petra SKAROUPKOVA**[†], **Ludek CERVENKA**[†][‡][§§] and
Vojtech MELENOVSKY[*][†][‡]

[*]Department of Cardiology, Institute for Clinical and Experimental Medicine (IKEM), Prague, Czech Republic, [†]Center for Experimental Medicine, Institute for Clinical and Experimental Medicine (IKEM), Prague, Czech Republic, [‡]Center for Cardiovascular Research, Prague, Czech Republic, [§]Institute of Physiology, Academy of Sciences of the Czech Republic, Prague, Czech Republic, [‖]Institute of Anatomy, 1st Faculty of Medicine, Charles University, Prague, Czech Republic, [¶]Institute of Molecular Genetics, Academy of Sciences of the Czech Republic, Prague, Czech Republic, [**]Institute of Pathological Physiology, 1st Faculty of Medicine, Charles University, Prague, Czech Republic, [††]Institute of Hematology and Blood Transfusion, Prague, Czech Republic, [‡‡]Institute of Microbiology v.v.i., Academy of Sciences of the Czech Republic, Prague, Czech Republic, and [§§]Department of Physiology, 2nd Faculty of Medicine, Charles University, Prague, Czech Republic.

A B S T R A C T

Advanced HF (heart failure) is associated with altered substrate metabolism. Whether modification of substrate use improves the course of HF remains unknown. The antihyperglycaemic drug MET (metformin) affects substrate metabolism, and its use might be associated with improved outcome in diabetic HF. The aim of the present study was to examine whether MET would improve cardiac function and survival also in non-diabetic HF. Volume-overload HF was induced in male Wistar rats by creating ACF (aortocaval fistula). Animals were randomized to placebo/MET (300 mg · kg^{-1} of body weight · day^{-1}, 0.5 % in food) groups and underwent assessment of metabolism, cardiovascular and mitochondrial functions ($n = 6$–12/group) in advanced HF stage (week 21). A separate cohort served for survival analysis ($n = 10$–90/group). The ACF group had marked cardiac hypertrophy, increased LVEDP (left ventricular end-diastolic pressure) and lung weight confirming decompensated HF, increased circulating NEFAs (non-esterified 'free' fatty acids), intra-abdominal fat depletion, lower glycogen synthesis in the skeletal muscle (diaphragm), lower myocardial triacylglycerol (triglyceride) content and attenuated myocardial ^{14}C-glucose and ^{14}C-palmitate oxidation, but preserved mitochondrial respiratory function, glucose tolerance and insulin sensitivity. MET therapy normalized serum NEFAs, decreased myocardial glucose oxidation, increased myocardial palmitate oxidation, but it had no effect on myocardial gene expression, AMPK (AMP-activated protein kinase) signalling, ATP level, mitochondrial respiration, cardiac morphology, function and long-term survival, despite reaching therapeutic serum levels (2.2 ± 0.7 μg/ml). In conclusion, MET-induced enhancement of myocardial fatty acid oxidation had a neutral effect on cardiac function and survival. Recently reported cardioprotective effects of MET may not be universal to all forms of HF and may require AMPK activation or ATP depletion. No increase in mortality on MET supports its safe use in diabetic HF.

INTRODUCTION

Advanced HF (heart failure) is characterized not only by a depression of heart mechanical performance, but also by altered myocardial metabolism, attenuated expression of fatty acid oxidation genes [1,2] and by diminished oxidation of long-chain fatty acids [1,3–5], which may contribute to diminished metabolic flexibility and to energetic deficiency that further promotes worsening of HF [6]. Targeting energetic substrate metabolism might thus serve as a target for novel therapeutic approaches to HF [7,8].

MET (metformin), a widely used antihyperglycaemic drug with insulin-sensitizing properties, could be a suitable candidate for metabolic HF therapy. MET lowers serum glucose by inhibiting liver gluconeogenesis, lowers circulating NEFAs (non-esterified 'free' fatty acids) and improves insulin sensitivity. Some effects of MET can be explained by an activation of AMPK (AMP-activated protein kinase) [9], the enzyme that senses and regulates cellular energetic homoeostasis, but it is not likely to be the only mechanism of MET effects [10,11]. Administration of MET might also favourably affect mitochondrial function and increase mitochondrial biogenesis by activating PPAR (peroxisome-proliferator-activated receptor)-α/PGC-1α (PPAR-γ coactivator-1α) [12]. Although MET is one of the most widely prescribed medications in human medicine, its effects on the heart are not well characterized.

Until recently, MET use in patients with HF was contraindicated due to a theoretical risk of lactic acidosis. Non-randomized observational studies had suggested that MET-treated diabetics with HF may have lower mortality than those on other antidiabetic regimes [13,14]. Because non-diabetic HF patients also have insulin resistance [15] and NEFA elevation [16], MET might be helpful in the wider HF population. The use of MET for metabolic therapy of HF needs to be established in experimental settings.

Volume overload represents a clinically relevant condition leading to HF, for example in aortic or mitral valve insufficiency. The rat model of chronic HF due to volume overload induced by ACF (aortocaval fistula) has been well characterized previously [17–19]. It shares many similarities with the natural course of human HF, including gradual development of the disease that proceeds through a stage of compensated hypertrophy followed by gradual decompensation into overt HF [19], neurohumoral activation, cardiac output redistribution [20], fluid retention with pulmonary congestion and impairment of myocardial efficiency [21]. On the other hand, volume-overload-induced HF has several features distinct from other HF models, including a lack of myocardial fibrosis and inflammation [22,23] and involvement of different signalling pathways (up-regulation of Akt and Wnt signalling) compared with experimental myocardial infarction or pressure overload [23]. The aim of the present study was to test the hypothesis that chronic MET therapy would correct HF-induced metabolic abnormalities and improve cardiac performance and survival in the volume-overload HF rat model.

MATERIALS AND METHODS

Animal HF model

HF was induced by volume overload from ACF using a needle technique [17,18]. Further details of the methods used can be found in the Supplementary Materials and methods section at http://www.clinsci.org/cs/121/cs1210029add.htm. Sham-operated controls underwent a similar procedure but without the creation of ACF. MET groups received 0.5 % MET (Teva Pharmaceuticals) mixed into the standard diet (normal salt/protein diet; 0.45 % NaCl, 19–21 % protein; SEMED), placebo (PL) groups received an identical diet but without MET. The study examined three rat cohorts, and each cohort had four randomly allocated groups: SH+PL (sham-operated without MET), SH+MET (sham-operated with MET), ACF+PL (ACF-without MET), ACF+MET (ACF with MET). The first cohort ($n = 6$–10/group) served for cardiac and mitochondrial function assessment, the second cohort ($n = 6$–8/group) served for organ metabolic studies and both cohorts were killed at week 21 after the ACF procedure. The third cohort ($n = 10$/SH groups, $n = 90$/ACF groups) was left free of any procedures and served for a survival analysis until week 52. The investigation conformed to the National Institutes of Health 'Guide for the care and use of laboratory animals' (NIH Publication no. 85–23, 1996) and Animal protection law of the Czech Republic (311/1997), and was approved by the ethics committee at IKEM.

Echocardiography and haemodynamics

Animals were anaesthetized i.p. (intraperitoneally) with a ketamine/midazolam injection (50 mg and 5 mg/kg of body weight). Echocardiography was performed using a 7.5 MHz probe (Vivid System 5, GE), and end-systolic and end-diastolic sizes of the left ventricle together with wall thicknesses were measured in PLAX (parasternal long-axis) and PSAX (parasternal short-axis) projection, the size of the right ventricle in A4C (apical four-chamber) projection. Invasive haemodynamic evaluation was performed by F2 Millar catheter inserted into the aorta and left ventricle via the carotid artery. After the haemodynamic assessment, rats were killed by exsanguination, the coronary tree was flushed with ice-cold cardioplegic solution and left ventricle free wall samples were instantly flash frozen in liquid nitrogen for

Myocardial biochemistry and ultrastructure

Myocardial ATP content was measured in flash-frozen tissue using HPLC [24]. The content of total and phosphorylated forms of AMPK was assessed by Western blotting as described previously [25]. Briefly, pAMPK (phosphorylated AMPK) was assessed using a rabbit anti-pAMPK antibody (Cell Signaling) and tAMPK (total AMPK) using a goat anti $\alpha1+\alpha2$ AMPK antibody (Santa Cruz Biotechnology). ACC (acetyl-CoA carboxylase) is a downstream target for AMPK. The ratio of pACC (phosphorylated ACC) at Ser79 to tACC (total ACC) is a robust assay of AMPK activation [26]. pACC was quantified by Western blotting using phospho-specific rabbit antibodies against Ser79 (Abcam). tACC was measured using IR-Dye-800-conjugated Streptavidine (Rockland). The mitochondrial respiratory chain complexes I–V were quantified by Western blotting [27]. Specific activities of cytochrome c oxidase and citrate synthase were determined spectrophotometrically in the myocardial homogenate [28]. Myocardial ultrastructure was studied on samples from the left ventricle fixed in glutaraldehyde, post-fixed with osmium tetroxide, stained with uranyl acetate and examined with a transmission electron microscope (Philips CM100l, FEI) with ×25 000 magnification. Image area occupied by mitochondria, myofibrils and cytoplasm was quantified using a grid point-counting method [29]; results are expressed as a percentage.

Mitochondrial function

In the myocardial tissue homogenate, the maximal ADP-stimulated oxidative capacity of mitochondria was determined as the oxygen consumption rate with palmitoylcarnitine (12.5 μM)+malate (3 mM)+glutamate (10 mM)+succinate (10 mM) using a high-resolution oxygraph-2k (OROBOROS) [30]. The respiratory control index, which indicates the tightness of the coupling between respiration and phosphorylation, was calculated as the ratio of glutamate+malate+ADP (1.5 mM) respiration without and with oligomycin (6 μM).

Myocardial gene expression

Total RNA was isolated by RNeasy Micro Kit (Qiagen), and 200 ng of total RNA was used for the amplification procedure and 1.5 μg of amplified RNA was hybridized on the chip according to the manufacturer's procedure.

Microarray analysis

The raw data (.TIFF image files) were analysed using 'beadarray' package [31] of the 'Bioconductor' [32] within the R environment (http://www.r-project.org) [33]. The GSEA (gene set enrichment analysis) was performed on gene sets defined by the KEGG (Kyoto Encyclopedia of Genes and Genomes; http://www.genome.ad.jp) pathways [34]. Lists of genes assigned to the KEGG pathways were downloaded from the KEGG (release 48.0).

Systemic and organ metabolic analyses

MET serum level was checked in tail-vein serum at week 11 in the ACF+MET ($n=12$) and SH+MET ($n=18$) groups. The MET level was measured using an HPLC method with separation on a silica column (ThermoQuest) with spectrophotometric detection. oGTTs (oral glucose tolerance tests) were performed in all groups at week 20 using an oral glucose load of 300 mg/100 g of body weight by gavage after overnight fasting. Blood was drawn from the tail without anaesthesia before the glucose load (0-min time point) and at 30, 60 and 120 min thereafter. Serum glucose was measured by the glucose-oxidase assay and serum NEFAs were determined using a colorimetric assay (Roche). Serum insulin was determined using a rat insulin ELISA kit (Mercodia). Tissue triacylglycerols were measured in liquid nitrogen-powdered tissues after chloroform/methanol extraction using the enzymatic assay (Pliva-Lachema); this assay was also used for serum triacylglycerols. The glycogen in the heart was measured after KOH extraction [35].

Glycogen synthesis and glucose oxidation in the heart and muscle

Basal and insulin-stimulated ^{14}C-glucose incorporation into glycogen and CO_2 was determined *ex vivo* in isolated diaphragm [36]. Similarly, 1-mm-thick cross-sectional slices of the left ventricle at midpapillary level were analysed [37].

Fatty acid oxidation in the heart

Fatty acid oxidation in the heart tissue muscles and heart slices was determined by measuring the incorporation of ^{14}C-palmitic acid into CO_2 [38].

Statistics

Two-way ANOVA with Bonferroni post-hoc adjustment was used to compare the effects of surgery and MET treatment. Survival analysis was performed using the Gehan–Breslow–Wilcoxon test. P values <0.05 were considered statistically significant.

RESULTS

MET serum assessment

MET serum level at week 11 was 2.2 ± 0.7 μg/ml (13 ± 4.15 nmol/ml) in the ACF+MET group ($n=12$) and 1.9 ± 2.7 μg/ml (11.6 ± 16.1 nmol/ml) in the

Table 1   Morphometric characteristics at week 21 after ACF

Values are means $\pm$ S.E.M., $n = 6$–8/group. BW, body weight; SH, sham-operated; PL, placebo. *Significantly different ($P < 0.05$) than sham.

Characteristic	Group			
	SH+PL	SH+MET	ACF+PL	ACF+MET
Body weight (g)	592 ± 20.9	603 ± 11.9	586 ± 23.4	579 ± 22.0
Heart weight (g)	1.63 ± 0.08	1.74 ± 0.04	3.10 ± 0.16*	3.23 ± 0.21*
Heart weight/BW (g/100 g)	2.80 ± 0.12	2.90 ± 0.12	5.29 ± 0.18*	5.59 ± 0.33*
Lung weight/BW (g/100 g)	3.30 ± 0.16	3.69 ± 0.53	4.23 ± 0.19*	4.48 ± 0.29*
Liver weight/BW (g/100 g)	28.7 ± 0.93	28.3 ± 0.99	27.7 ± 1.01	27.0 ± 1.04
Tibia length (mm)	43.2 ± 0.30	42.3 ± 0.41	43.1 ± 0.43	43.1 ± 0.42
Epididymal fat body/BW (g/100 g)	1.63 ± 0.16	1.46 ± 0.14	1.22 ± 0.06*	1.30 ± 0.11*
Perirenal fat body/BW (g/100 g)	1.52 ± 0.17	1.41 ± 0.24	1.05 ± 0.08*	1.25 ± 0.11*
Subcutaneous fat body/BW (g/100 g)	0.26 ± 0.04	0.28 ± 0.02	0.26 ± 0.12	0.25 ± 0.09

Table 2   Haemodynamics at week 21 after ACF

Values are means $\pm$ S.E.M., $n = 6$–8/group. LV, left ventricular; SH, sham-operated; PL, placebo. *Significantly different ($P < 0.05$) than sham.

Parameter	Group			
	SH+PL	SH+MET	ACF+PL	ACF+MET
Maximal LV pressure (mmHg)	129 ± 7.11	139 ± 8.33	120 ± 3.96	128 ± 6.94
LVEDP (mmHg)	6.7 ± 0.84	6.8 ± 0.45	12.1 ± 0.66*	11.4 ± 1.35*
Systolic duration (% of cycle duration)	46.7 ± 4.79	49.5 ± 1.77	59.8 ± 1.95*	55.3 ± 1.21*
Heart rate (s^{-1})	345 ± 13.3	386 ± 10.3	360 ± 10.8	323 ± 13.3
dP/dt_{max} (mmHg/s)	11417 ± 965	12730 ± 834	11504 ± 733	11655 ± 1030
dP/dt_{min} (mmHg/s)	− 13314 ± 1593	− 12520 ± 4192	− 11056 ± 2540	− 11508 ± 1977
LV relaxation constant tau (s)	0.015 ± 0.0013	0.012 ± 0.0013	0.034 ± 0.0188	0.039 ± 0.0203

SH+MET group ($n = 18$; $P = 0.68$), being within the range of human therapeutic dose (corresponding to a daily 2000 mg of MET dose in an average adult; http://www.accessdata.fda.gov/drugsatfda_docs/label/2008/020357s031,021202s016lbl.pdf) and within the range of no observable adverse effect for rats [40].

Organ morphometry, haemodynamics and echocardiography

All groups had similar body weights and tibial lengths. Both ACF groups had marked heart hypertrophy (Table 1) and increased lung weight/body weight indicating pulmonary congestion. ACF animals had a depletion of intra-abdominal adipose tissue in epididymal and perirenal fat bodies.

ACF animals had elevated LVEDP (left ventricular end-diastolic pressure), indicating decompensated heart failure, but still preserved left ventricular contractility (dP/dt_{max}) and relaxation (dP/dt_{min}, tau constant). The systolic duration/cycle length ratio was higher in both ACF groups. No effect of MET on haemodynamics was observed (Table 2).

ACF animals had marked enlargement of both ventricles (Table 3), a 2-fold increase in stroke volume and cardiac output due to fistula and diminished left ventricular fractional shortening and LVEF (left ventricular ejection fraction). Both left ventricular anterior and posterior walls in all groups showed similar thicknesses. No effect of MET on echocardiographic parameters was observed.

Metabolic assessment

Glucose and glycogen metabolism

When assessed using oGTTs, all the groups showed similar glucose levels throughout the test and preserved postprandial glycaemic regulation (Figures 1A and 1B). ACF animals had lower insulin levels at the baseline (Figure 1C) and a trend towards lower levels postload (Figure 1D). Myocardium of all animals showed similar contents of glycogen (Figure 2D) and rate of glycogen synthesis (results not shown). Myocardial glucose oxidation was significantly lower in both ACF groups, and MET treatment induced further lowering (Figure 2E), independently of the ACF procedure. ACF animals had a lower rate of glycogen synthesis

Table 3 Echocardiography at week 21 after ACF

Values are means ± S.E.M., $n = 6$–8/group. LV, left ventricular; RV, right ventricular; SH, sham-operated; PL, placebo.
*Significantly different ($P < 0.05$) than sham.

Parameter	Group			
	SH+PL	SH+MET	ACF+PL	ACF+MET
Heart rate (s^{-1})	425 ± 12.3	432 ± 12.7	370 ± 27.4	375 ± 18.2
LV diastolic diameter (mm)	6.08 ± 0.40	6.70 ± 0.09	10.20 ± 0.48*	9.75 ± 0.40*
LV systolic diameter (mm)	1.95 ± 0.42	2.63 ± 0.19	5.47 ± 0.42*	4.62 ± 0.39*
LV fractional shortening (%)	69.2 ± 5.00	60.8 ± 2.78	46.7 ± 2.46*	53.0 ± 2.58*
LV anterior wall thickness in diastole (mm)	2.30 ± 0.08	2.28 ± 0.07	2.33 ± 0.09	2.25 ± 0.09
LV posterior wall thickness in diastole (mm)	2.33 ± 0.07	2.32 ± 0.09	2.31 ± 0.09	2.23 ± 0.12
RV diastolic diameter (mm)	2.85 ± 0.18	3.34 ± 0.30	5.07 ± 0.29*	4.96 ± 0.52*
LVEF (%)	93.0 ± 2.36	88.6 ± 1.72	75.2 ± 2.66*	81.4 ± 2.56*
Stroke volume (μl)	174 ± 21.6	205 ± 7.07	447 ± 44.6*	436 ± 35.3*
Cardiac output (ml/min)	73.57 ± 8.6	88.80 ± 4.7	159.85 ± 10.8*	160.41 ± 9.2

in the skeletal muscle (diaphragm) than sham animals (Figure 3A), but all groups had a similar insulin-stimulated increment of glycogen synthesis (Figure 3B), which is a measure of skeletal muscle insulin sensitivity [36,41]. There was no difference in skeletal muscle (diaphragm) glucose oxidation (results not shown).

Lipid metabolism

Serum and liver triacylglycerols were similar in all groups (Figures 2A and 2C). In contrast, myocardial triacylglycerol content was markedly decreased in ACF animals (Figure 2B). ACF animals had increased serum NEFA concentrations in fasted state and even more after glucose loading compared with sham-operated animals. MET treatment reduced NEFA levels in both MET-treated groups compared with placebo (Figures 1E and 1F). Myocardial palmitate oxidation was reduced in the ACF+PL group by 37% ($P < 0.001$) compared with SH+PL. MET treatment (ACF+MET) increased myocardial palmitate oxidation to a level similar to that in the SH+PL group (Figure 2F).

Mitochondrial function

Cytochrome c oxidase (complex IV) and citrate synthase activities (Figures 5D and 5E) and the protein content of mitochondrial respiratory chain complexes I–V did not show any difference between groups (Supplementary Figure S1 at http://www.clinsci.org/cs/121/cs1210029add.htm). Maximal ADP-stimulated respiratory chain capacity, measured as O_2 consumption with palmitoyl-carnitine+malate+glutamate+succinate (Figure 5C), as well as respiratory control index (Figure 5B), was again similar in all groups, reflecting that the resting respiration was largely intact and coupled. Analysis of myocardial ATP content showed a similar level of ATP (Figure 5A), indicating an undisturbed resting energetic state in HF animals.

Electron microscopy showed no apparent structural abnormalities, and the proportions occupied by myofibrils, mitochondria and cytosol were similar in all groups (Supplementary Figure S2 at http://www.clinsci.org/cs/121/cs1210029add.htm).

AMPK signalling

To characterize the activity of the AMPK-regulatory cascade, total content and phosphorylation of both AMPK and its target ACC were assessed by Western blotting. At the level of AMPK, ACF animals showed significantly higher contents of both tAMPK and pAMPK than sham groups. However, the ratio between pAMPK and tAMPK (pAMPK/tAMPK) was similar, independent of ACF procedure or MET treatment (Figures 4A–4C). At the level of ACC, no differences either in tACC, pACC or in pACC/tACC ratio were observed between groups (Figures 4D–4F). These results suggest a modest upstream AMPK activation due to ACF procedure, but the absence of a significant functional consequence at the level of the downstream target of AMPK either due to ACF procedure or to MET treatment.

Myocardial gene expression analysis

Out of 23 401 detected transcripts, we observed no difference between ACF+MET and ACF+PL, which was in striking contrast with fistula-induced transcriptional changes (ACF+PL compared with SH+PL), where 128 transcripts were differentially expressed (99 up-regulated and 29 down-regulated; Storey's q value <0.05 and 2-fold or greater change in intensity). A heatmap with all differentially expressed transcripts is shown in Supplementary Figure S3 (http://www.clinsci.org/cs/121/cs1210029add.htm). KEGG pathway analysis revealed the down-regulation of pathways involved in fatty acid metabolism in response
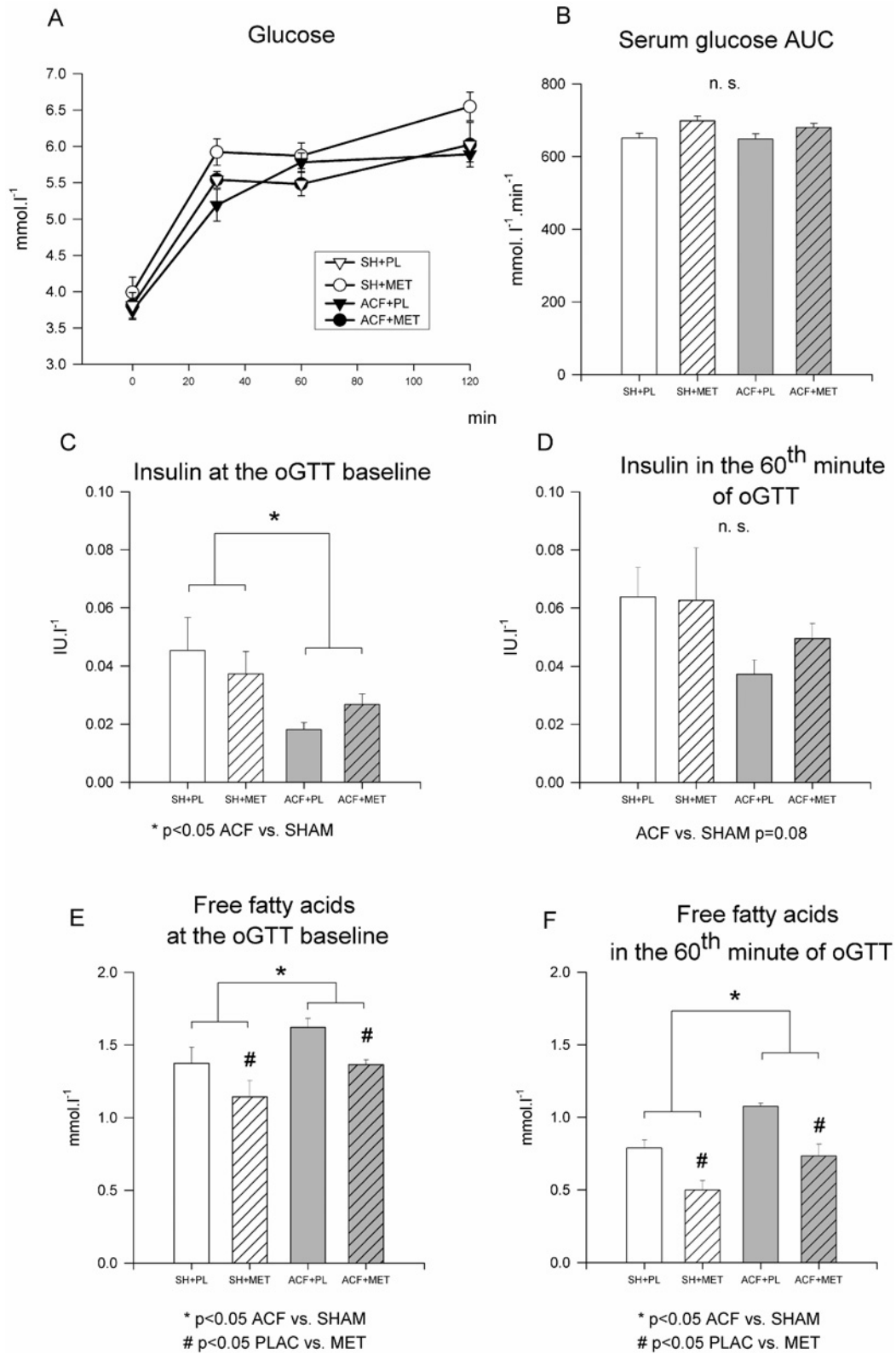
Figure 1   Serum levels of glucose, NEFAs and insulin

(A) Serum glucose levels during oGTT. (B) AUC (area under the curve) of serum glucose during oGTT. (C) Serum insulin level at the beginning of oGTT. (D) Serum insulin level at 60 min of oGTT. (E) Serum NEFAs at the beginning of oGTT. (F) Serum NEFAs at 60 min of oGTT. Results are expressed as means $\pm$ S.E.M. n.s., not significant.
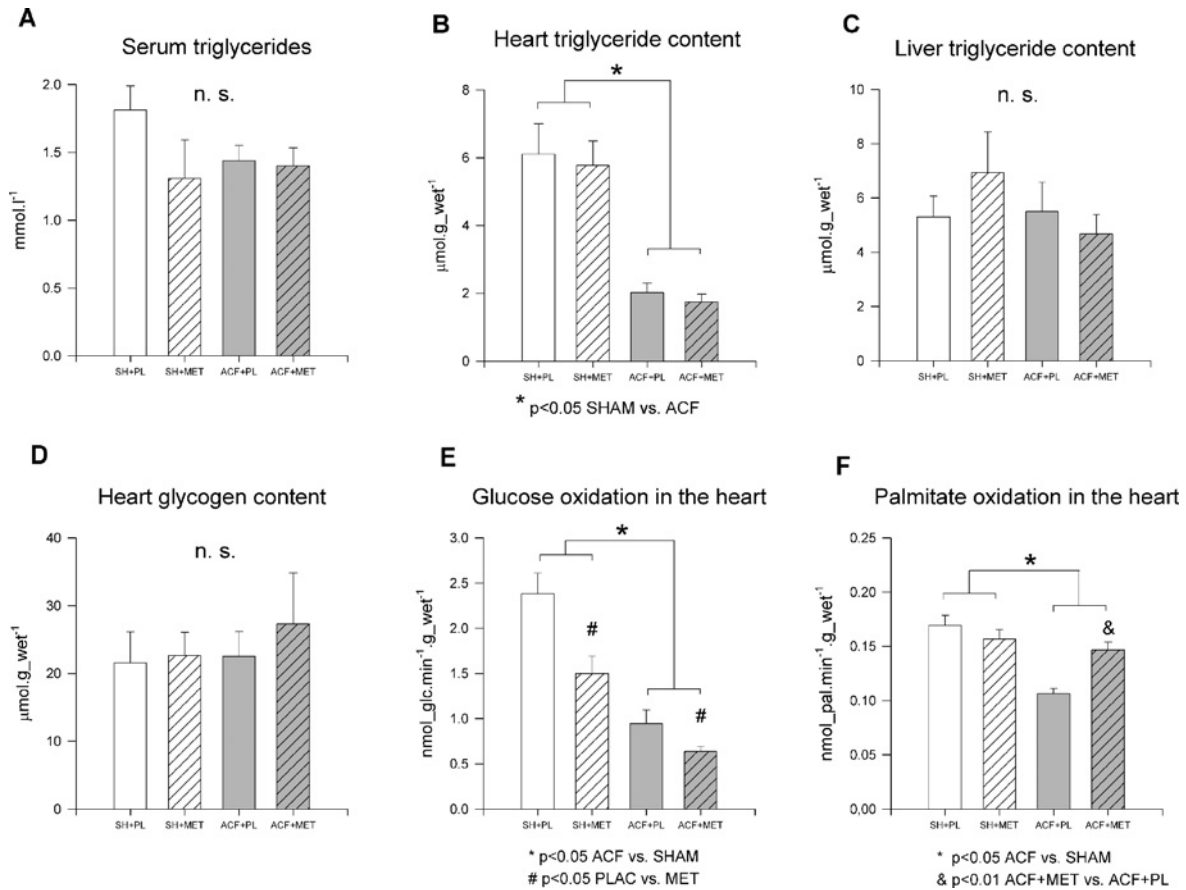
Figure 2   Content and metabolism of lipids and glucose

(A) Triacylglycerols (triglycerides) in the serum. (B) Triacylglycerols in the heart. (C) Triacylglycerols in the liver. (D) Glycogen in the heart. (E) ^{14}C-glucose oxidation in the heart. (F) ^{14}C-palmitate oxidation in the heart. Results are expressed as means $\pm$ S.E.M. n.s., not significant.
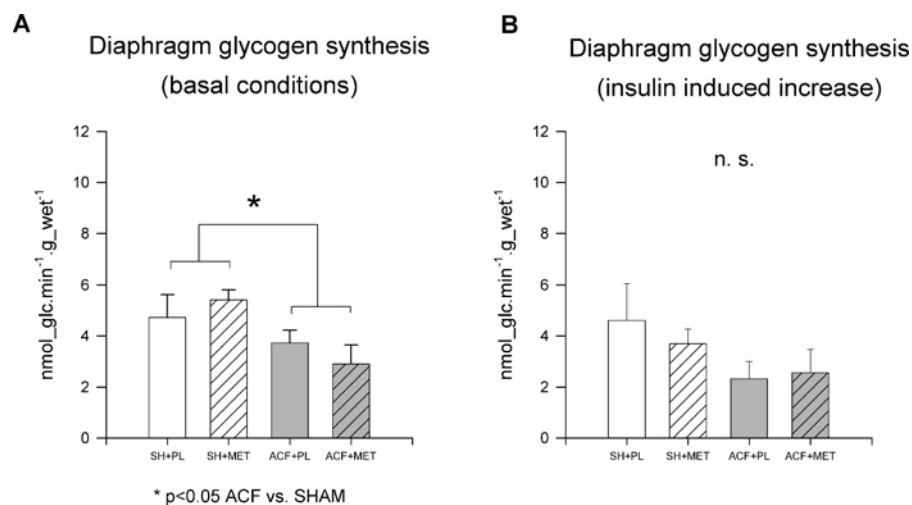
Figure 3   Diaphragm glycogen synthesis

(A) Diaphragm glycogen synthesis under basal conditions. (B) Diaphragm glycogen synthesis; increase in glycogen synthesis due to insulin stimulation. Results are expressed as means $\pm$ S.E.M. n.s., not significant.
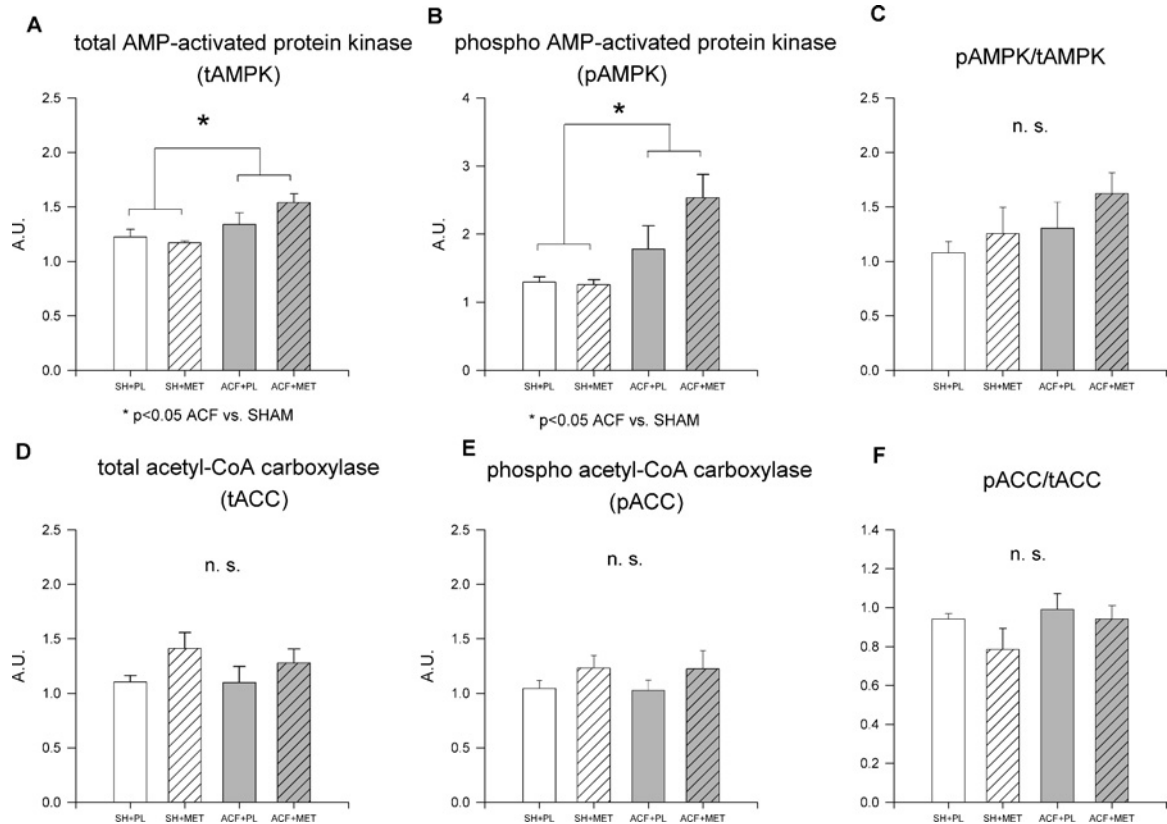
Figure 4   Heart AMPK activation

(A) tAMPK. (B) pAMPK. (C) Ratio between pAMPK and tAMPK. (D) tACC. (E) pACC. (F) Ratio between pACC and tACC. Results are expressed as means $\pm$ S.E.M. A.U., arbitrary units n.s., not significant.

to ACF (Supplementary Table S1 http://www.clinsci.org/cs/121/cs1210029add.htm).

Survival

None of the control animals died throughout the study. The first deaths in the ACF groups occurred between weeks 10 and 15, and 77.2 % of the ACF+PL (80.5 % of ACF+MET) animals were dead by the end of the study. Median survival was 45.5 weeks in the ACF+PL group and 44.5 weeks in the ACF+MET group. MET therapy had no effect on survival in ACF animals (Figure 6).

DISCUSSION

The present study shows that chronic volume overload-induced HF is associated with lower glycogen synthesis in the skeletal muscle (diaphragm), lower heart triacylglycerol content, higher plasma NEFAs, lower plasma insulin level and depressed myocardial glucose and palmitate oxidation. Long-term administration of the antihyperglycaemic drug MET normalized elevated NEFAs, further decreased myocardial glucose oxidation and increased myocardial palmitate oxidation, but had

no effect on myocardial AMPK activation, ATP content, mitochondrial function or morphology. No relevant improvement in cardiac performance or long-term survival was observed in MET-treated HF animals. Despite several recent studies reported beneficial effect of MET in other non-diabetic HF models [42–44], our present study indicates that this improvement is not common to all HF forms. Decreased cellular energetic charge [10] and/or AMPK activation by MET may be required for improvement of cardiac performance in HF. Conversely, prolonged exposure of symptomatic HF animals to high-dose MET led to no increase in mortality, supporting safety of MET use in diabetic HF.

Peripheral and systemic MET effects

At the systemic level, MET lowered basal and post-prandial circulating NEFAs due to increased NEFA utilization and perhaps also due to diminished NEFA release from adipose tissue because of known inhibitory effects of MET on catecholamine-stimulated lipolysis [45]. ACF rats had a depletion of intra-abdominal adipose tissue, indicative of enhanced fat mobilization due to neurohumoral activation from HF, but MET did not reverse fat depletion. MET also had no effect on
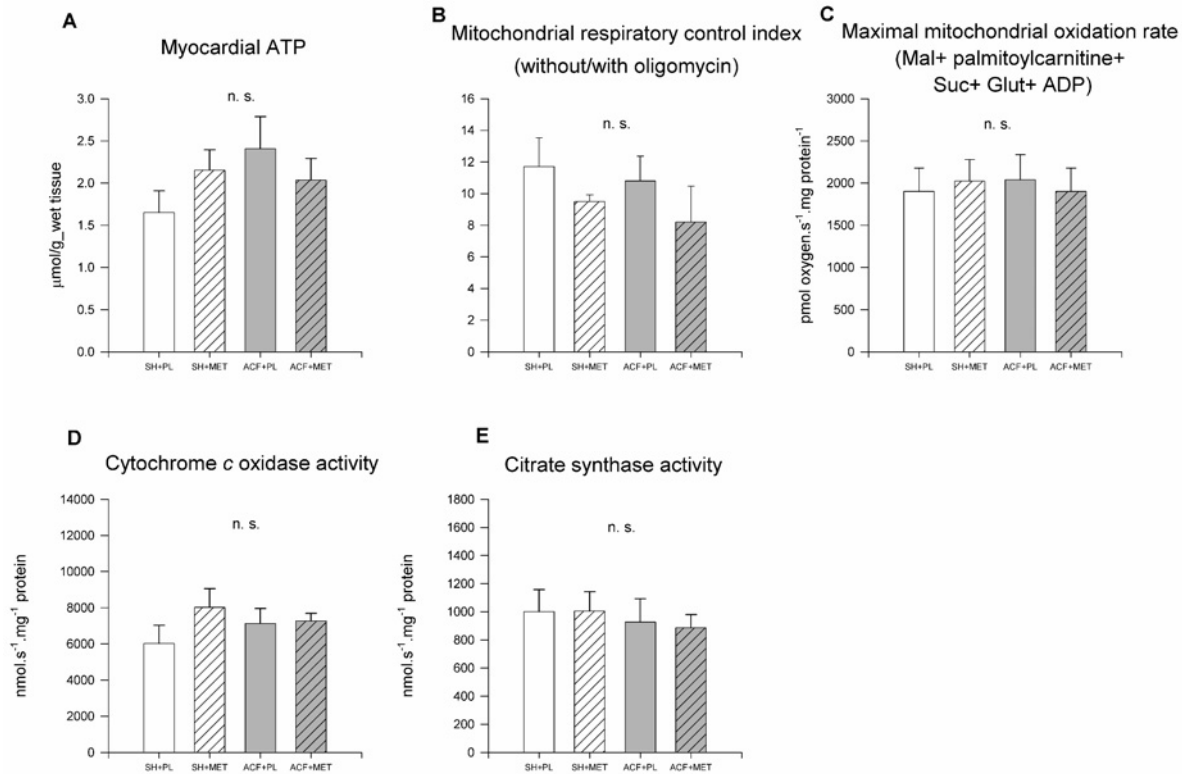
Figure 5 Mitochondrial function
(A) ATP content. (B) Mitochondrial respiratory control index (with glutamate, without/with oligomycin). (C) Maximal mitochondrial oxidation rate (with malate, palmitoylcarnitine, succinate, glutamate and ADP). (D) Cytochrome *c* oxidase activity. (E) Citrate synthase activity. Results are expressed as means $\pm$ S.E.M. n.s., not significant.
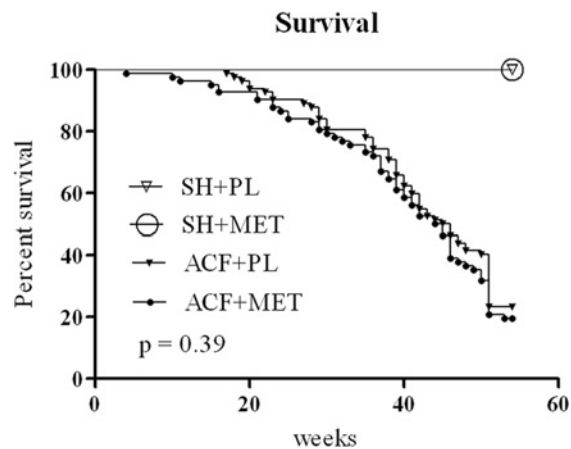
Figure 6 Survival analysis

insulin-mediated glycogen synthesis in skeletal muscle, which is a measure of insulin sensitivity.

Cardiac effects of MET

In the heart, MET treatment significantly increased the palmitate oxidation that was attenuated in the ACF+PL group. Diminished oxidation of long-chain

fatty acids and down-regulation of enzymes of fatty acid oxidation in the heart have been repeatedly described both in HF patients [1] and in animal HF models [3,4,46], including rats with ACF [5,47,48], reflecting probably a reactivation of a fetal-like gene transcriptional programme [2,4]. Whether this change is adaptive or not is still under discussion. The functional consequences of drug-induced reversal of diminished fatty acid oxidation are unknown. Our present study indicates that drug-induced enhancement of fatty acid oxidation has a neutral effect on survival and cardiac function in HF due to volume overload, supporting the view that diminished myocardial fatty acid oxidation does not play a causal role in HF progression. Similar findings were reported also in pacing-induced HF, where long-term therapy with the PPAR-α agonist fenofibrate increased fatty acid utilization, but did not delay HF onset [49]. MET had no effect on mitochondrial respiratory function, myocardial gene transcription profile and the size of the mitochondrial compartment within the cardiomyocyte, speaking against the specific activation of mitochondrial biogenesis [50]. Myocardial gene expression profile in MET-treated ACF animals was unchanged, indicating non-genomic mechanisms involved in the fatty acid oxidation increase after MET. Moravec and co-workers

[5] have shown that isolated cardiac mitochondria from ACF rats have impaired activation and transport of the palmitoyl group across the outer mitochondrial membrane (via palmitoyl-CoA synthase and carnitine palmitoyl-CoA transferase-1), leading to attenuated oxidation of palmitate, but preserved oxidation of palmitoyl carnitine. Kinetic studies indicated that the co-operation between those two enzymes deteriorates with increasing NEFA concentrations. Thus the improvement in fatty acid oxidation after MET treatment in ACF group can be a consequence of the mere reduction of circulating NEFAs in serum [5]. The apparent opposite responses of myocardial fatty acid oxidation and glucose oxidation can be explained either by a MET-induced inhibition of glycolysis [11] or by a Randle effect, i.e., increased fatty acid oxidation increases the concentration of acetyl-CoA in the Krebs cycle, leading to an inhibition of pyruvate dehydrogenase with a subsequent inhibition of glycolysis and glucose oxidation [51].

Comparison with other HF studies

The absence of benefit of MET on cardiac function or survival in ACF-induced HF is in contrast with other recently published studies in other HF models. Gundewar et al. [44] examined the effect of very low dose MET (125 μg·kg^{-1} of body weight·day^{-1}, i.p.) on cardiac function and survival in mice subjected to LAD (left anterior descending coronary artery) ligation. MET extended the survival at 4 weeks by 47%, improved left ventricular remodelling and corrected MI (myocardial infarction)-induced defects in mitochondrial respiration and ATP synthesis. Despite the fact that the administered MET dose was lower by three orders of magnitude than in our present study (i.e. 300 mg of MET·kg^{-1} of body weight·day^{-1}) or than is normally used in humans, authors were able to detect increased phosphorylation of AMPK, eNOS (endothelial NO synthase) and increased expression of PGC-1α in the heart. In another study, Sasaki et al. [42] examined the effect of 4-week oral MET therapy (100 mg·kg^{-1} of body weight·day^{-1}) in the tachypacing HF model in dogs. Compared with placebo, MET improved LVEF, slowed HF progression and decreased myocardial apoptosis via an AMPK-dependent mechanism [42]. Xiao et al. [52] documented an improvement in cardiac diastolic function upon MET treatment in a pressure overload HF model. The dose used in that study (200 mg·kg^{-1} of body weight·day^{-1}) was similar to ours.

Lack of a protecting effect of MET in a volume-overload HF model

The mechanism of MET action is still incompletely understood. One possibility suggests an activation of AMPK that turns on energy-providing and turns off energy-consuming metabolic pathways [9,53], but non-AMPK-dependent MET effects have also been described [10,11]. The reason why MET therapy provided no haemodynamic or survival benefit in the ACF-induced HF model in contrast with other models is not clear. We excluded the possibility of underdosing or poor absorption because MET serum levels were adequate and within the therapeutic range observed in humans [40]. The effect of MET could be affected by varying intracellular import, which depends on the capacity of OCT-1 (organic cation transporter-1). Genetic polymorphisms in the OCT-1 gene (SCL22A1) were shown to affect a clinical response to MET therapy in humans [54]. In our present study, MET administration had no effect on either mitochondrial functions or on mitochondrial and ultrastructural morphology. Ultrastructural morphology was similar among groups regardless of ACF procedure or MET treatment, despite a marked increase in heart weights in both ACF groups. This can be explained by an increase in myocyte width and length [55]. An increase in both pAMPK and tAMPK forms of AMPK was observed, with a preserved pAMPK/tAMPK ratio. On the level of ACC, which is a direct downstream target of AMPK, no differences in pACC, tACC or in the pACC/tACC ratio occurred. This observation suggests a modest upstream AMPK activation due to ACF procedure, but the absence of a significant functional consequence at the level of the downstream target of AMPK. Insufficient AMPK activation could potentially explain the lack of MET benefit in our model. AMPK catalytic subunits are highly conserved, so interspecies structural differences are unlikely to explain the inability of MET to activate AMPK in our protocol. An absence of AMPK activation in our ACF-induced HF model could be explained by an unaltered myocardial ATP level in this model. Model-specific differences thus seem to provide an acceptable explanation. The cardioprotective effect of MET can be at least partially ascribed to the attenuation of cardiac fibrosis [52], but compared with pre-ssure overload, volume overload is not associated with increased myocardial fibrosis [22,23]. Compared with the study by Gundewar et al. [44], we did not find any increase in AMPK activity or decrease in oxygen consumption rate or respiratory control index. It appears that in contrast with pressure overload, volume overload does not sufficiently alter resting mitochondrial function [23], and thus, it may lack the substrate for MET action. Finally, no insulin resistance was observed in our volume-overload HF model, so the lack of insulin resistance might also imply a missing substrate for MET action. Despite all these specifics of the model, we should be aware that HF is a non-uniform syndrome, and it should be studied in subsets. Volume overload is a clinically important condition, and its most common form (mitral insufficiency) often complicates other heart diseases and independently increases mortality [56].

Metabolic abnormalities in the ACF HF model

The ACF-induced HF model showed several specific features. Despite gene expression analysis showing an extensive down-regulation of the β-oxidation pathway and several respiratory chain components in ACF, the ATP-generating capacity of mitochondria in surplus oxygen and substrates was preserved. This might be explained by a redundancy in enzyme activities and longer half-life [4,57]. Myocardial ATP content, presented for the first time in this model, was also normal. This is in agreement with the study from Marcil et al. [58] who showed normal myocardial oxidative capacity in compensated ACF-induced HF (week 15), but marked sensitivity of the heart to hypoxia, indicating preserved ATP levels at rest, but attenuated energetic reserve during increased stress. Low myocardial triacylglycerol content in ACF hearts, also reported for the first time, is probably related to limited re-esterification of triacylglycerols due to low availability of NADPH [59], and this abnormality was unchanged by MET therapy. Although a number of works described connections between elevated levels of NEFAs [16] and insulin resistance [15,60] in HF, muscle insulin sensitivity, measured as an insulin-induced increment of glycogen synthesis [36,41], was preserved in ACF, making perhaps this model less prone to the benefits of MET. Interestingly, fasting and postprandial insulinaemia were actually lower in ACF than in control animals. Pancreatic hypoperfusion or negative effects of chronically elevated NEFAs on pancreatic β-cell secretory function might be responsible for this phenomenon [61].

In conclusion, the results of the present study show that long-term MET therapy in rats with HF due to volume overload decreases circulating NEFAs, decreases myocardial glucose oxidation and increases myocardial palmitate oxidation, but these effects have neutral impact on cardiac performance and survival in HF. Recently reported cardioprotective effects of MET may not be universal to all forms of HF and may require AMPK activation or ATP depletion. Prolonged exposure of a large group of severely symptomatic HF animals to high-dose MET led to no apparent increase in mortality, which provides robust data regarding the toxicology of MET [40] and supports its safe use in HF patients with diabetes.

AUTHOR CONTRIBUTION

Jan Benes, Vojtech Melenovsky, Ludek Cervenka and Ludmila Kazdova designed the study, analysed the data and drafted the manuscript; Vojtech Melenovsky, Jan Benes and Petra Skaroupkova carried out the animal work, echocardiography and haemodynamics; David Sedmera and Oldrich Benada performed the electron microscopy; Ludmila Kazdova and Jiri Petrak conducted the biochemical and metabolic studies; Hynek Strand, Jan Kopecky and Michal Kolar performed the gene expression analyses; Zdenek Drahota, Josef Houstek, Dasa Medrikova, Jan Kopecky, Nikola Kovarova and Marek Vrbacky performed the mitochondrial function analyses and determined the heart ATP levels.

REFERENCES

1 Razeghi, P., Young, M. E., Alcorn, J. L., Moravec, C. S., Frazier, O. H. and Taegtmeyer, H. (2001) Metabolic gene expression in fetal and failing human heart. Circulation **104**, 2923–2931

2 Sack, M. N., Rader, T. A., Park, S., Bastin, J., McCune, S. A. and Kelly, D. P. (1996) Fatty acid oxidation enzyme gene expression is downregulated in the failing heart. Circulation **94**, 2837–2842

3 Doenst, T., Pytel, G., Schrepper, A., Amorim, P., Farber, G., Shingu, Y., Mohr, F. W. and Schwarzer, M. (2009) Decreased rates of substrate oxidation *ex vivo* predict the onset of heart failure and contractile dysfunction in rats with pressure overload. Cardiovasc. Res. **86**, 461–470

4 van Bilsen, M., van Nieuwenhoven, F. A. and Van Der Vusse, G. J. (2009) Metabolic remodelling of the failing heart: beneficial or detrimental? Cardiovasc. Res. **81**, 420–428

5 Christian, B., Alaoui-Talibi, Z., Moravec, M. and Moravec, J. (1998) Palmitate oxidation by the mitochondria from volume-overloaded rat hearts. Mol. Cell Biochem. **180**, 117–128

6 Neubauer, S. (2007) The failing heart: an engine out of fuel. N. Engl. J. Med. **356**, 1140–1151

7   Ashrafian, H., Frenneaux, M. P. and Opie, L. H. (2007)
    Metabolic mechanisms in heart failure. Circulation **116**,
    434–448

8   Lee, L., Campbell, R., Scheuermann-Freestone, M.,
    Taylor, R., Gunaruwan, P., Williams, L., Ashrafian, H.,
    Horowitz, J., Fraser, A. G., Clarke, K. and Frenneaux, M.
    (2005) Metabolic modulation with perhexiline in chronic
    heart failure: a randomized, controlled trial of short-term
    use of a novel treatment. Circulation **112**, 3280–3288

9   Zhou, G., Myers, R., Li, Y., Chen, Y., Shen, X.,
    Fenyk-Melody, J., Wu, M., Ventre, J., Doebber, T., Fujii, N.
    et al. (2001) Role of AMP-activated protein kinase in
    mechanism of metformin action. J. Clin. Invest. **108**,
    1167–1174

10 Foretz, M., Hebrard, S., Leclerc, J., Zarrinpashneh, E.,
    Soty, M., Mithieux, G., Sakamoto, K., Andreelli, F. and
    Viollet, B. (2010) Metformin inhibits hepatic
    gluconeogenesis in mice independently of the
    LKB1/AMPK pathway via a decrease in hepatic energy
    state. J. Clin. Invest. **120**, 2355–2369

11 Saeedi, R., Parsons, H. L., Wambolt, R. B., Paulson, K.,
    Sharma, V., Dyck, J. R., Brownsey, R. W. and Allard, M. F.
    (2008) Metabolic actions of metformin in the heart can
    occur by AMPK-independent mechanisms. Am. J. Physiol.
    Heart Circ. Physiol. **294**, H2497–H2506

12 Suwa, M., Egashira, T., Nakano, H., Sasaki, H. and
    Kumagai, S. (2006) Metformin increases the PGC-1α
    protein and oxidative enzyme activities possibly via AMPK
    phosphorylation in skeletal muscle *in vivo*. J. Appl.
    Physiol. **101**, 1685–1692

13 Eurich, D. T., Majumdar, S. R., McAlister, F. A., Tsuyuki,
    R. T. and Johnson, J. A. (2005) Improved clinical outcomes
    associated with metformin in patients with diabetes and
    heart failure. Diabetes Care **28**, 2345–2351

14 Masoudi, F. A., Inzucchi, S. E., Wang, Y., Havranek, E. P.,
    Foody, J. M. and Krumholz, H. M. (2005)
    Thiazolidinediones, metformin, and outcomes in older
    patients with diabetes and heart failure: an observational
    study. Circulation **111**, 583–590

15 Doehner, W., Rauchhaus, M., Ponikowski, P., Godsland,
    I.F., von Haehling, S., Okonko, D. O., Leyva, F., Proudler,
    A. J., Coats, A. J. and Anker, S. D. (2005) Impaired insulin
    sensitivity as an independent risk factor for mortality in
    patients with stable chronic heart failure. J. Am. Coll.
    Cardiol. **46**, 1019–1026

16 Lommi, J., Kupari, M. and Yki-Jarvinen, H. (1998) Free
    fatty acid kinetics and oxidation in congestive heart failure.
    Am. J. Cardiol. **81**, 45–50

17 Garcia, R. and Diebold, S. (1990) Simple, rapid, and
    effective method of producing aortocaval shunts in the rat.
    Cardiovasc. Res. **24**, 430–432

18 Brower, G. L. and Janicki, J. S. (2001) Contribution of
    ventricular remodeling to pathogenesis of heart failure in
    rats. Am. J. Physiol. Heart Circ. Physiol. **280**, H674–H683

19 Brower, G. L., Henegar, J. R. and Janicki, J. S. (1996)
    Temporal evaluation of left ventricular remodeling and
    function in rats with chronic volume overload. Am. J.
    Physiol. **271**, H2071–H2078

20 Flaim, S. F., Minteer, W. J., Nellis, S. H. and Clark, D. P.
    (1979) Chronic arteriovenous shunt: evaluation of a model
    for heart failure in rat. Am. J. Physiol. **236**, H698–H704

21 Takewa, Y., Chemaly, E.R., Takaki, M., Liang, L.F., Jin, H.,
    Karakikes, I., Morel, C., Taenaka, Y., Tatsumi, E. and
    Hajjar, R. J. (2009) Mechanical work and energetic analysis
    of eccentric cardiac remodeling in a volume overload heart
    failure in rats. Am. J. Physiol. Heart Circ. Physiol. **296**,
    H1117–H1124

22 Ruzicka, M., Keeley, F. W. and Leenen, F. H. (1994) The
    renin–angiotensin system and volume overload-induced
    changes in cardiac collagen and elastin. Circulation **90**,
    1989–1996

23 Toischer, K., Rokita, A.G., Unsold, B., Zhu, W.,
    Kararigas, G., Sossalla, S., Reuter, S.P., Becker, A., Teucher,
    N., Seidler, T. et al. (2010) Differential cardiac remodeling
    in preload versus afterload. Circulation **122**, 993–1003

24 Argaud, D., Roth, H., Wiernsperger, N. and Leverve, X.M.
    (1993) Metformin decreases gluconeogenesis by enhancing
    the pyruvate kinase flux in isolated rat hepatocytes. Eur. J.
    Biochem. **213**, 1341–1348

25 Kus, V., Prazak, T., Brauner, P., Hensler, M., Kuda, O.,
    Flachs, P., Janovska, P., Medrikova, D., Rossmeisl, M.,
    Jilkova, Z. et al. (2008) Induction of muscle thermogenesis
    by high-fat diet in mice: association with obesity-
    resistance. Am. J. Physiol. Endocrinol. Metab. **295**,
    E356–E367

26 Hutber, C. A., Hardie, D. G. and Winder, W. W. (1997)
    Electrical stimulation inactivates muscle acetyl-CoA
    carboxylase and increases AMP-activated protein kinase.
    Am. J. Physiol. **272**, E262–E266

27 Mracek, T., Pecinova, A., Vrbacky, M., Drahota, Z. and
    Houstek, J. (2009) High efficiency of ROS production by
    glycerophosphate dehydrogenase in mammalian
    mitochondria. Arch. Biochem. Biophys. **481**, 30–36

28 Drahota, Z., Milerova, M., Stieglerova, A., Houstek, J. and
    Ostadal, B. (2004) Developmental changes of cytochrome c
    oxidase and citrate synthase in rat heart homogenate.
    Physiol. Res. **53**, 119–122

29 Nouette-Gaulain, K., Malgat, M., Rocher, C., Savineau,
    J.P., Marthan, R., Mazat, J. P. and Sztark, F. (2005) Time
    course of differential mitochondrial energy metabolism
    adaptation to chronic hypoxia in right and left ventricles.
    Cardiovasc. Res. **66**, 132–140

30 Pecina, P., Capkova, M., Chowdhury, S. K., Drahota, Z.,
    Dubot, A., Vojtiskova, A., Hansikova, H., Houst'kova, H.,
    Zeman, J., Godinot, C. and Houstek, J. (2003) Functional
    alteration of cytochrome *c* oxidase by SURF1
    mutations in Leigh syndrome. Biochim. Biophys. Acta
    1639, 53–63

31 Dunning, M. J., Smith, M. L., Ritchie, M. E. and Tavare, S.
    (2007) beadarray: R classes and methods for Illumina
    bead-based data. Bioinformatics **23**, 2183–2184

32 Gentleman, R. C., Carey, V. J., Bates, D. M., Bolstad, B.,
    Dettling, M., Dudoit, S., Ellis, B., Gautier, L., Ge, Y.,
    Gentry, J. et al. (2004) Bioconductor: open software
    development for computational biology and
    bioinformatics. Genome Biol. **5**, R80

33 Strnad, H., Lacina, L., Kolar, M., Cada, Z., Vlcek, C.,
    Dvorankova, B., Betka, J., Plzak, J., Chovanec, M.,
    Sachova, J. et al. (2010) Head and neck squamous cancer
    stromal fibroblasts produce growth factors influencing
    phenotype of normal human keratinocytes. Histochem.
    Cell. Biol. **133**, 201–211

34 Kanehisa, M. and Goto, S. (2000) KEGG: Kyoto
    Encyclopedia of Genes and Genomes. Nucleic Acids Res.
    28, 27–30

35 Cahova, M., Vavrinkova, H., Meschisvilli, E., Markova, I.
    and Kazdova, L. (2004) The impaired response of
    non-obese hereditary hypertriglyceridemic rats to glucose
    load is associated with low glucose storage in energy
    reserves. Exp. Clin. Endocrinol. Diabetes **112**, 549–555

36 Cahova, M., Vavrinkova, H., Tutterova, M., Meschisvilli,
    E. and Kazdova, L. (2003) Captopril enhanced insulin-
    stimulated glycogen synthesis in skeletal muscle but not
    fatty acid synthesis in adipose tissue of hereditary
    hypertriglyceridemic rats. Metab. Clin. Exp. **52**, 1406–1412

37 Russell, III, R. R., Bergeron, R., Shulman, G. I. and
    Young, L. H. (1999) Translocation of myocardial GLUT-4
    and increased glucose uptake through activation of AMPK
    by AICAR. Am. J. Physiol. **277**, H643–H649

38 Sugimoto, K., Kazdova, L., Qi, N. R., Hyakukoku, M., Kren, V., Simakova, M., Zidek, V., Kurtz, T. W. and Pravenec, M. (2008) Telmisartan increases fatty acid oxidation in skeletal muscle through a peroxisome proliferator-activated receptor-γ dependent pathway. J. Hypertens. **26**, 1209–1215

39 Reference deleted

40 Quaile, M. P., Melich, D. H., Jordan, H. L., Nold, J. B., Chism, J. P., Polli, J. W., Smith, G. A. and Rhodes, M. C. (2010) Toxicity and toxicokinetics of metformin in rats. Toxicol. Appl. Pharmacol. **243**, 340–347

41 Kraegen, E. W., Jenkins, A. B., Storlien, L. H. and Chisholm, D. J. (1990) Tracer studies of *in vivo* insulin action and glucose metabolism in individual peripheral tissues. Horm. Metab. Res. Suppl. **24**, 41–48

42 Sasaki, H., Asanuma, H., Fujita, M., Takahama, H., Wakeno, M., Ito, S., Ogai, A., Asakura, M., Kim, J., Minamino, T. et al. (2009) Metformin prevents progression of heart failure in dogs: role of AMP-activated protein kinase. Circulation **119**, 2568–2577

43 Calvert, J. W., Gundewar, S., Jha, S., Greer, J. J., Bestermann, W. H., Tian, R. and Lefer, D. J. (2008) Acute metformin therapy confers cardioprotection against myocardial infarction via AMPK–eNOS-mediated signaling. Diabetes **57**, 696–705

44 Gundewar, S., Calvert, J. W., Jha, S., Toedt-Pingel, I., Ji, S. Y., Nunez, D., Ramachandran, A., Anaya-Cisneros, M., Tian, R. and Lefer, D. J. (2009) Activation of AMP-activated protein kinase by metformin improves left ventricular function and survival in heart failure. Circ. Res. **104**, 403–411

45 Zhang, T., He, J., Xu, C., Zu, L., Jiang, H., Pu, S., Guo, X. and Xu, G. (2009) Mechanisms of metformin inhibiting lipolytic response to isoproterenol in primary rat adipocytes. J. Mol. Endocrinol. **42**, 57–66

46 Stanley, W. C., Recchia, F. A. and Lopaschuk, G. D. (2005) Myocardial substrate metabolism in the normal and failing heart. Physiol. Rev. **85**, 1093–1129

47 Alaoui-Talibi, Z., Landormy, S., Loireau, A. and Moravec, J. (1992) Fatty acid oxidation and mechanical performance of volume-overloaded rat hearts. Am. J. Physiol. **262**, H1068–H1074

48 Ben Cheikh, R., Guendouz, A. and Moravec, J. (1994) Control of oxidative metabolism in volume-overloaded rat hearts: effects of different lipid substrates. Am. J. Physiol. **266**, H2090–H2097

49 Labinskyy, V., Bellomo, M., Chandler, M. P., Young, M. E., Lionetti, V., Qanud, K., Bigazzi, F., Sampietro, T., Stanley, W. C. and Recchia, F. A. (2007) Chronic activation of peroxisome proliferator-activated receptor-α with fenofibrate prevents alterations in cardiac metabolic phenotype without changing the onset of decompensation in pacing-induced heart failure. J. Pharmacol. Exp. Ther. **321**, 165–171

50 Kukidome, D., Nishikawa, T., Sonoda, K., Imoto, K., Fujisawa, K., Yano, M., Motoshima, H., Taguchi, T., Matsumura, T. and Araki, E. (2006) Activation of AMP-activated protein kinase reduces hyperglycemia-induced mitochondrial reactive oxygen species production and promotes mitochondrial biogenesis in human umbilical vein endothelial cells. Diabetes **55**, 120–127

51 Randle, P. J., Garland, P. B., Hales, C. N. and Newsholme, E. A. (1963) The glucose fatty-acid cycleIts role in insulin sensitivity and the metabolic disturbances of diabetes mellitus. Lancet **i**, 785–789

52 Xiao, H., Ma, X., Feng, W., Fu, Y., Lu, Z., Xu, M., Shen, Q., Zhu, Y. and Zhang, Y. (2010) Metformin attenuates cardiac fibrosis by inhibiting the TGFβ1-Smad3 signalling pathway. Cardiovasc. Res. **87**, 504–513

53 Wong, A. K., Howie, J., Petrie, J. R. and Lang, C. C. (2009) AMP-activated protein kinase pathway: a potential therapeutic target in cardiometabolic disease. Clin. Sci. **116**, 607–620

54 Becker, M. L., Visser, L. E., van Schaik, R. H., Hofman, A., Uitterlinden, A. G. and Stricker, B. H. (2009) Genetic variation in the organic cation transporter 1 is associated with metformin response in patients with diabetes mellitus. Pharmacogenomics J. **9**, 242–247

55 Benes, Jr, J., Melenovsky, V., Skaroupkova, P., Pospisilova, J., Petrak, J., Cervenka, L. and Sedmera, D. (2011) Myocardial morphological characteristics and proarrhythmic substrate in the rat model of heart failure due to chronic volume overload. Anat. Rec. **294**, 102–111

56 Ling, L. H., Enriquez-Sarano, M., Seward, J. B., Tajik, A. J., Schaff, H. V., Bailey, K. R. and Frye, R. L. (1996) Clinical outcome of mitral regurgitation due to flail leaflet. N. Engl. J. Med. **335**, 1417–1423

57 Morgan, E. E., Chandler, M. P., Young, M. E., McElfresh, T. A., Kung, T. A., Rennison, J. H., Tserng, K. Y., Hoit, B. D. and Stanley, W. C. (2006) Dissociation between gene and protein expression of metabolic enzymes in a rodent model of heart failure. Eur. J. Heart Failure **8**, 687–693

58 Marcil, M., Ascah, A., Matas, J., Belanger, S., Deschepper, C. F. and Burelle, Y. (2006) Compensated volume overload increases the vulnerability of heart mitochondria without affecting their functions in the absence of stress. J. Mol. Cell. Cardiol. **41**, 998–1009

59 Pound, K. M., Sorokina, N., Ballal, K., Berkich, D. A., Fasano, M., Lanoue, K. F., Taegtmeyer, H., O'Donnell, J. M. and Lewandowski, E. D. (2009) Substrate–enzyme competition attenuates upregulated anaplerotic flux through malic enzyme in hypertrophied rat heart and restores triacylglyceride content: attenuating upregulated anaplerosis in hypertrophy. Circ. Res. **104**, 805–812

60 Swan, J. W., Anker, S. D., Walton, C., Godsland, I. F., Clark, A. L., Leyva, F., Stevenson, J. C. and Coats, A. J. (1997) Insulin resistance in chronic heart failure: relation to severity and etiology of heart failure. J. Am. Coll. Cardiol. **30**, 527–532

61 Bollheimer, L. C., Skelly, R.H., Chester, M. W., McGarry, J. D. and Rhodes, C. J. (1998) Chronic exposure to free fatty acid reduces pancreatic beta cell insulin content by increasing basal insulin secretion that is not compensated for by a corresponding increase in proinsulin biosynthesis translation. J. Clin. Invest. **101**, 1094–1101

Effect of metformin therapy on cardiac function and survival in a volume-overload model of heart failure in rats

Jan BENES*†‡, **Ludmila KAZDOVA**†, **Zdenek DRAHOTA**§, **Josef HOUSTEK**§,
Dasa MEDRIKOVA§, **Jan KOPECKY**§, **Nikola KOVAROVA**§, **Marek VRBACKY**§,
David SEDMERA§‖, **Hynek STRNAD**¶, **Michal KOLAR**¶, **Jiri PETRAK****††,
Oldrich BENADA‡‡, **Petra SKAROUPKOVA**†, **Ludek CERVENKA**†‡§§ and
Vojtech MELENOVSKY*†‡

*Department of Cardiology, Institute for Clinical and Experimental Medicine (IKEM), Prague, Czech Republic, †Center for Experimental Medicine, Institute for Clinical and Experimental Medicine (IKEM), Prague, Czech Republic, ‡Center for Cardiovascular Research, Prague, Czech Republic, §Institute of Physiology, Academy of Sciences of the Czech Republic, Prague, Czech Republic, ‖Institute of Anatomy, 1st Faculty of Medicine, Charles University, Prague, Czech Republic, ¶Institute of Molecular Genetics, Academy of Sciences of the Czech Republic, Prague, Czech Republic, **Institute of Pathological Physiology, 1st Faculty of Medicine, Charles University, Prague, Czech Republic, ††Institute of Hematology and Blood Transfusion, Prague, Czech Republic, ‡‡Institute of Microbiology v.v.i., Academy of Sciences of the Czech Republic, Prague, Czech Republic, and §§Department of Physiology, 2nd Faculty of Medicine, Charles University, Prague, Czech Republic.

SUPPLEMENTARY MATERIALS AND METHODS

Chronic HF model from volume overload

HF was induced by volume overload from ACF using a needle technique [1–3]. Male Wistar rats (Anlab) weighting 300–350 g were anaesthetized with ketamine/midazolam mixture (5 mg of midazolam and 50 mg of ketamine/kg of body weight) and midline abdominal laparotomy was performed to expose the infrarenal aorta and vena cava. An 18-gauge needle (diameter 1.2 mm; Becton Dickinson) was inserted into the abdominal aorta and advanced through the medial wall into the vena cava to create ACF as described previously [1–3]. The aorta above the puncture was then temporarily clamped, needle withdrawn and the puncture site was sealed with cyanacrylate glue. Creation of ACF was confirmed by observing pulsatile, bright flow in the inferior vena cava. The abdominal cavity was closed by an absorbable suture. The ACF procedure was associated with 13 % early ($\leqslant$7 days) mortality, occurring mostly within the first 48 h.

After 1 week, animals were randomly divided into MET and placebo groups. MET groups received 0.5 % MET (Teva Pharmaceuticals) in food (normal salt/protein diet–0.45 % NaCl, 19–21 % protein; SEMED), calculated intake from preliminary experiments was 300 mg · kg^{-1} of body weight · day^{-1}. Placebo groups received the same, but without the addition of MET. All animals were kept on a 12/12-h light/dark cycle and were weighted weekly. Three different rat cohorts were employed in the study; in each cohort, four different types of rats were present: SH+PL (sham-operated without MET), SH+MET (sham-operated with MET), ACF+PL (ACF without MET) and ACF+MET (ACF with MET). The first cohort of rats ($n = 6$–10) served for an echocardiography analysis, invasive haemodynamic analysis, gene transcription analysis, transmission electron microscopy analysis, mitochondrial function analysis, AMPK signalling analysis and ATP content analysis. The second rat cohort ($n = 6$–8) served for a metabolic analysis. The third rat cohort ($n = 10$ for SH+PL and SH+MET, $n = 90$ for ACF+PL and ACF+MET) served for a survival analysis. Sample size calculation ($n = 70$) was based on a mortality assumption by week 30 of 50 % in the no-treatment group and 29 % in the treated group (log-rank test, one-sided, $\alpha = 0.05$, $\beta = 0.8$) with some reserve ($n = 20$/group) for early surgical mortality. Since rats survived the procedure better than expected, all surviving animals were left in the experiment in order to avoid an underpowered study.

Except for the survival analysis, all experiments were carried out at week 21. Animals that died up to week 21 were excluded from the analysis. No animals were excluded from the survival analysis cohort.

Correspondence: Dr Jan Benes (email jan.benes@ikem.cz).

Echocardiography and haemodynamics

All measurements were performed at the study end (week 21). Animals were anaesthetized with an above-mentioned mixture of ketamine/midazolam i.p. injection, shaved, and ventricular thicknesses and dimensions were measured in triplicate by an experienced echocardiographer using a 7.5 MHz US probe (Vivid System 5, GE). End-systolic and end-diastolic left ventricular volumes were derived by cubic equation [4] and the stroke volume as their difference. After echocardiography, invasive haemodynamics evaluation was performed by Millar micromanometer catheter inserted into the aorta and left ventricle via the carotid artery. Pressure and three-lead ECG signal were digitalized at 1 kHz and recorded using a Powerlab 8 platform for off-line analysis with LabChart software (ADInstruments). The presence of pulsatile AVF was then verified from midline laparotomy, and the animals were killed by rapid exsanguination. The beating heart was excised, and the coronary tree was promptly orthogradely perfused with 10 ml of ice-cold St Thomas cardioplegia solution. The apical part of the left ventricle was used for the assessment of AMPK signalling, ATP content analysis and mitochondrial function analysis. The basal third of the ventricles was used for morphology. Midventricular samples of left ventricular free wall were immediately harvested into RNA-Later solution (Ambion) and stored at $-80\,^{\circ}$C. Wet weights of liver, kidney and lungs were measured in wet state and normalized to body weight.

Transmission electron microscopy

Ultrastructural studies were performed on samples fixed in 3.25% (v/v) glutaraldehyde in cacodylate buffer, postfixed in osmium tetroxide and embedded in epoxy resin. Ultrathin sections were cut (Leica EM UC6) and stained with uranyl acetate and Reynolds solution. Sections were imaged with a Phillips CM100 electron microscope (FEI). Individual images were recorded at a primary magnification of ×25000 and 80 kV. Digital image acquisition was carried out with MegaViewII slow scan camera resolution of 1280 × 1024 pixels and 12 bits dynamic range. For high-resolution imaging of large sample areas, a MIA module of Analysis 3.2 software was used. This module allows automatic image recording using the image shift function and subsequent image stitching. MIA module parameters were the following: every high resolution overview image was created from a matrix of 4 × 5 images (1280 × 1024 px each) with 96 pixels overlap. Resulting high-resolution images were trimmed and equalized by standard module functions. Subsequently, the final images were processed using the DCE filter of the Analysis 3.2 system in order to enhance the rendition of mitochondrial membrane system. The proportion of mitochondrial and myofibrillar volume was estimated on electron micrographs using a standard stereological point counting method (e.g. Gundersen and

Jensen [4a]). Digital micrographs were opened in Adobe Photoshop (version 8.0) and overlayed by a 250 × 250 pixel grid using the Show ⟶ Grid option. Using three separate layers (for mitochondria, myofibrils and the rest of the cytoplasm excluding nuclei), dots were placed over the grid line intercepts with each particular structure of interest using a Pencil tool. The number of dots in each layer was then automatically counted after exporting the individual layers as uncompressed TIFF files in ImageJ. Mitochondrial and myofibrillar fractions were then defined as a percentage of intercepts of these structures from total cell volume, as described previously [5].

Gene expression and GSEA (gene set enrichment analysis) pathway analysis

RNA analysis

Total RNA was isolated by an RNeasy Micro Kit (Qiagen) according to the procedure for fibrous tissues (cardiomyocytes). The quantity of the RNA was measured on a NanoDrop ND-1000 (NanoDrop Technologies LLC). RNA integrity was assessed on an Agilent 2100 Bioanalyser (Agilent Technologies). All RNA samples had RIN (RNA integrity number) >8. Illumina RatRef-12 v1 Expression BeadChip (Illumina) was used for the microarray analysis following the standard protocol: 200 ng of total RNA was amplified with Illumina TotalPrep RNA Amplification Kit (Ambion) and 1.5 μg of amplified RNA was hybridized on the chip according to the manufacturer's procedure. All analyses were done in $\geqslant 6$ individual animals per group.

Microarray analysis

The raw data (.TIFF image files) were analysed using 'beadarray' package [6] of the 'Bioconductor' [7] within the R environment (http://www.r-project.org) [8]. All hybridizations passed a control of quality. The data were background-corrected, variance-stabilized by logarithmic transformation and normalized with the probe level quantile method. Before detection of differential expression, 50% of the least varying probes based on IQR (interquantile range) were disregarded; however, the probes with detection P value <0.05 in at least one sample (null model: negative controls of the BeadChip) were kept. Analysis of differential expression was performed with the 'limma' package [9]. Annotation of differentially expressed transcripts was done against the manifest provided by Illumina (RatRef_12_V1_0_R3_11222119_A.bgx; Illumina). Only transcripts with Storey's q-value <0.05 [10] and fold-change <0.5 or >2 were reported. The data were deposited in the ArrayExpress database (accession no. E-MTAB-190).

Pathway analysis

GSEA was performed on gene sets defined by the KEGG pathways [11]. Lists of genes assigned to the KEGG pathways were downloaded from the KEGG (release 48.0) directly, and the probes were assigned to KEGG pathways accordingly. Two methods of GSEA were applied: first, we performed a simple Fischer test on over-representation of up-regulated (respectively, down-regulated, significantly changed) probes in a selected KEGG pathway against the overall ratio of up-regulated (down-regulated, significantly changed) probes in the complete dataset. Secondly, we performed GSEA according to Tian et al. [12]. Only pathways with a false discovery rate [13] <0.05 are reported in the present study.

Determination of ATP content

Flash-frozen heart tissues stored in liquid nitrogen were extracted by homogenization in 6% (w/v) perchloric acid (0.5 ml of solution per 100 mg of tissue). After centrifugation for 10 min at 4°C and 10000 g, the supernatants were neutralized (final pH of 6–7) with 0.4 M triethanolamine+1.8 M KOH. ATP concentration was determined using the HPLC procedure as described [14]. Separation and quantification was performed using a Hewlett-Packard 1100 system with a diode array detector. Calibration was performed using the appropriate standards.

Quantification of ACC

Tissue lysates (10 μg of protein) were subjected to electrophoresis using precast 3–8% Tris/acetate gels (Invitrogen). Protein was transferred to nitrocellulose membranes (Bio-Rad), and the membranes were blocked in Odyssey Blocking Buffer (Li-Cor Biosciences) for 1 h at RT (room temperature; 22°C). Phospho-specific rabbit antibodies against the Ser[79] (Abcam) site on ACC were used (incubation overnight at 4°C) for the detection of pACC (phosphorylated ACC) and IR Dye 800 conjugated Streptavidine (Rockland) for the detection of the tACC (total ACC) (incubation overnight at 4°C). After overnight incubation, membranes labelled with antibody against pACC were washed 5 × 5 min with TBST [TBS (Tris-buffered saline) containing 0.1% Tween 20] and then incubated for 1 h at RT with secondary antibody (anti-rabbit IgG conjugated to IR dye 800; Rockland). After incubation, membranes were washed 5 × 5 min using TBST and 1 × 5 min with TBS. Then, membranes were scanned using Odyssey IR Imager (Li-Cor Biosciences). Results were evaluated with Aida software.

Quantification of AMPK

The content of tAMPK and pAMPK was assessed by Western blot as described before [15]. Tissue lysates (15 μg protein) were subjected to SDS/PAGE (10% gel). Protein was transferred to NC Hybond C-extra membrane (Amersham Biosciences), and the membranes were blocked in Odyssey Blocking Buffer (Li-Cor Biosciences) for 1 h at RT. Primary antibodies against phospho-AMPK (rabbit anti-pAMPK; Cell Signaling Technology) and tAMPK (goat anti-α1+α2 AMPK; Santa Cruz Biotechnology) were used. After overnight incubation, membranes labelled with antibodies against AMPK and pAMPK were washed 5 × 5 min with TBST and then incubated for 1 h at RT with secondary antibody (anti-goat IgG conjugated to IR dye700 and anti-rabbit IgG conjugated to IR dye800; Rockland). After incubation, membranes were washed for 5 × 5 min using TBST and once for 10 min with TBS. Then, membranes were scanned using Odyssey IR Imager (Li-Cor Biosciences). Results were evaluated with Aida software.

Mitochondrial function assessments

Tissue samples of the left ventricle (50–100 mg wet weight) were cut by scissors on ice into small pieces and gently homogenized using a Teflon-glass homogenizer at 4°C in 25 mM sucrose, 75 mM sorbitol, 100 mM KCl, 5 mM MgCl$_2$, 10 mM Tris/HCl, 0.05 mM EDTA, pH 7.2 and filtered through 200-μm nylon mesh. In homogenates, the quantity of mitochondrial respiratory chain complexes was determined by electrophoretic analysis combined with immunoblotting using specific antibodies as described before [16]. Specific activities of cytochrome c oxidase and citrate synthase in the homogenate were determined spectrophotometrically [17]. Maximal ADP-stimulated oxidative capacity of mitochondria in the homogenate was determined as oxygen consumption rate with palmitoyl carnitine (12.5 μM)+malate (3 mM)+glutamate (10 mM)+succinate (10 mM) using high-resolution oxygraph-2k (OROBOROS) [18], and the respiratory control index was calculated as the ratio of glutamate+malate+ADP (1.5 mM)–respiration without and with oligomycin (6 μM).

Metabolic analyses

Biochemical analyses

Blood glucose levels were measured by the glucose oxidase assay (Pliva-Lachema) using tail vein blood drawn into 5% trichloroacetic acid and promptly centrifuged. Serum NEFA levels were determined using an acyl-CoA oxidase-based colorimetric kit (Roche Diagnostics).

Tissue triacylglycerol measurements

For the determination of triacylglycerol in the heart, tissues were powdered under liquid nitrogen and extracted for 16 h in chloroform/methanol (2:1, v/v), after which 2% KH$_2$PO$_4$ was added, and the solution was centrifuged. The organic phase was removed and evaporated under N$_2$. The resulting pellet was
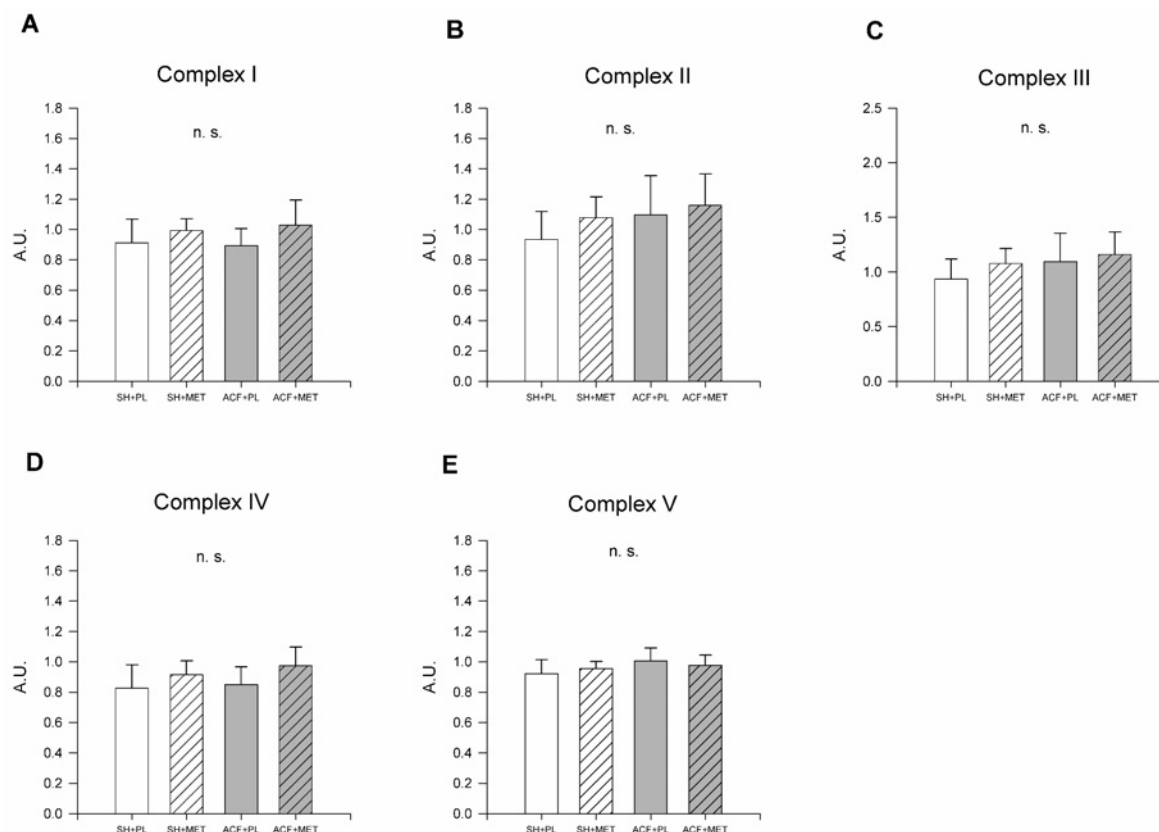
Figure S1 Mitochondrial respiratory chain protein complexes show no difference in their abundance (results) between the animals with ACF and the controls

(A) Mitochondrial protein complex I, (B) complex II, (C) complex III, (D) complex IV and (E) complex V. Results are from the Western blot analysis and are expressed as means $\pm$ S.E.M. A. U., arbitrary units; n.s., not significant.

dissolved in propan-1-ol, and triacylglycerol content was determined by an enzymatic assay (Pliva-Lachema).

Glycogen content in myocardium

The glycogen from the heart was extracted by boiling in 30% KOH and reprecipitated three times with 96% ethanol. The precipitate was centrifuged, washed with ethanol, and the content of glycogen was determined as described previously [19].

Muscle and myocardial glycogen synthesis and glucose oxidation

Basal and insulin-stimulated ^{14}C-U-glucose incorporation into glycogen and CO_2 was determined *ex vivo* in isolated diaphragm and heart slices as described previously [20,21]. Briefly, after decapitation, tissues were incubated for 2 h in Krebs–Ringer bicarbonate buffer, at 37°C, gas phase 95% O_2+5% CO_2, pH 7.4, that contained 5.5 mM unlabelled glucose, 0.1 μCi/ml of ^{14}C-U-glucose and 3 mg/ml BSA (Armour, Fraction V) with or without 250 μ-units/ml insulin. All incubations were performed at 37°C in sealed vials in a shaking water bath.

After 2-h incubation, 0.3 ml of 1 M hyamine hydroxide was injected into the central compartment of the incubation vessel and 0.5 ml of 1 M H_2SO_4 into the main compartment to liberate CO_2. The vessels were incubated for another 45 min; the hyamine hydroxide was then quantitatively transferred into the scintillation vial containing scintillation fluid for the counting of radioactivity.

For the measurement of basal and insulin-stimulated glucose incorporation into glycogen, muscles were removed from the incubation medium, rinsed in ice-cold physiological solution and put into chloroform/methanol (2:1, v/v). Myocardial muscle metabolism was measured by a modified method reported elsewhere [22]. Instead of isolated papillary muscles, 1-mm thick cross-sectional slices of the left ventricle at midpapillary level were analysed to provide higher mass and signal.

Fatty acid oxidation in cardiac muscle

Fatty acid oxidation was determined in heart slices by measuring the incorporation of palmitic acid into CO_2 as described previously [23]. Palmitate oxidation was measured in Krebs–Ringer bicarbonate buffer with
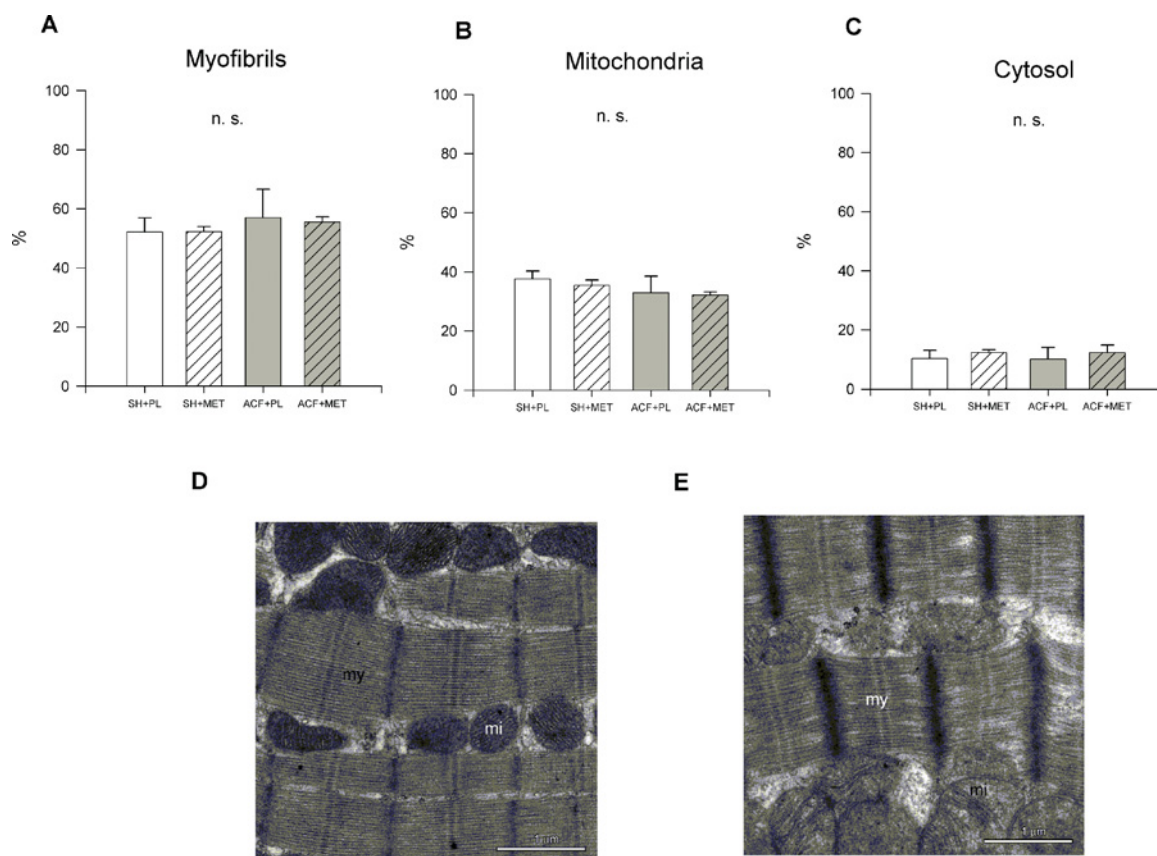
Figure S2   Transmission electron microscopy shows no differences between the animals with ACF and the controls

Proportions of (A) myofibrils (my), (B) mitochondria (mi) and (C) cytosol in the study groups. Results are expressed as means $\pm$ S.E.M. (D) Electron micrograph of a representative ACF+MET sample and (E) electron micrograph of a representative SH+MET sample.

0.5 μCi/ml of ^{14}C-palmitic acid complexed with BSA (3 mg/ml, fraction V; Sigma) and 0.3 μmol/ml cold (non-radioactive) palmitic acid. The incubation was carried out at 37 °C in sealed vials in a shaking water bath. After a 2-h incubation, 0.2 ml of 1.0 M hyamine hydroxide was injected into the central compartment of the vessel, and 0.5 ml of 1 M H_2SO_4 was injected into the main compartment containing incubation medium to liberate CO_2. The vessels were incubated for an additional 45 min. The hyamine hydroxide was then quantitatively transferred to the scintillation vial for radioactivity counting. Results are expressed as nmol of palmitate $\cdot$ min^{-1} $\cdot$ g^{-1} of wet tissue.

Assessment of MET serum levels

The concentrations of MET were determined using an HPLC method with spectrophotometric detection. The serum samples were stored in the freezer at -80 °C. Thawing was allowed at RT before processing of the sample. A portion (25 μl) of serum were pipetted to the tube, and 150 μl of acetonitrile was added. No internal standard was used. The tube was vortex-mixed for 30 s at 400 g. The tube was then

centrifuged for 3 min at 600 g, and the supernatant was transferred to the autosampler vial. Five microlitres was injected into a HPLC system consisting of the P1000 pump, UV 1000 spectrophotometric detector, data station with PC1000 software, version 2.5 (Thermo Separation Products) and Midas automatic sample injector (Spark Holland). The separation was performed on a Hypersil Silica 30 mm × 4.6 mm, 3 μm column (ThermoQuest, Hypersil Division) with a silica 4 mm × 3 mm precolumn (Phenomenex, Torrance). The mobile phase consisted of acetonitrile/10 mM ammonium acetate mixture (60:40, v/v). The flow rate was 1 ml/min at 35 °C. The analyte retention time was 2.4 min at these conditions, and the whole run time lasted 3 min. The detection wavelength was 238 nm, and the time constant of the detector was set to 0.5 s.

The autosampler was operated in a pickup mode with acetonitrile used as the transport liquid. The wash solution in the autosampler was methanol/water/acetic acid mixture (50:50:1). The calibration curve was constructed from six points in the range 93.65–5277 ng/ml to encompass the expected concentrations in measured samples. The calibration curves were obtained
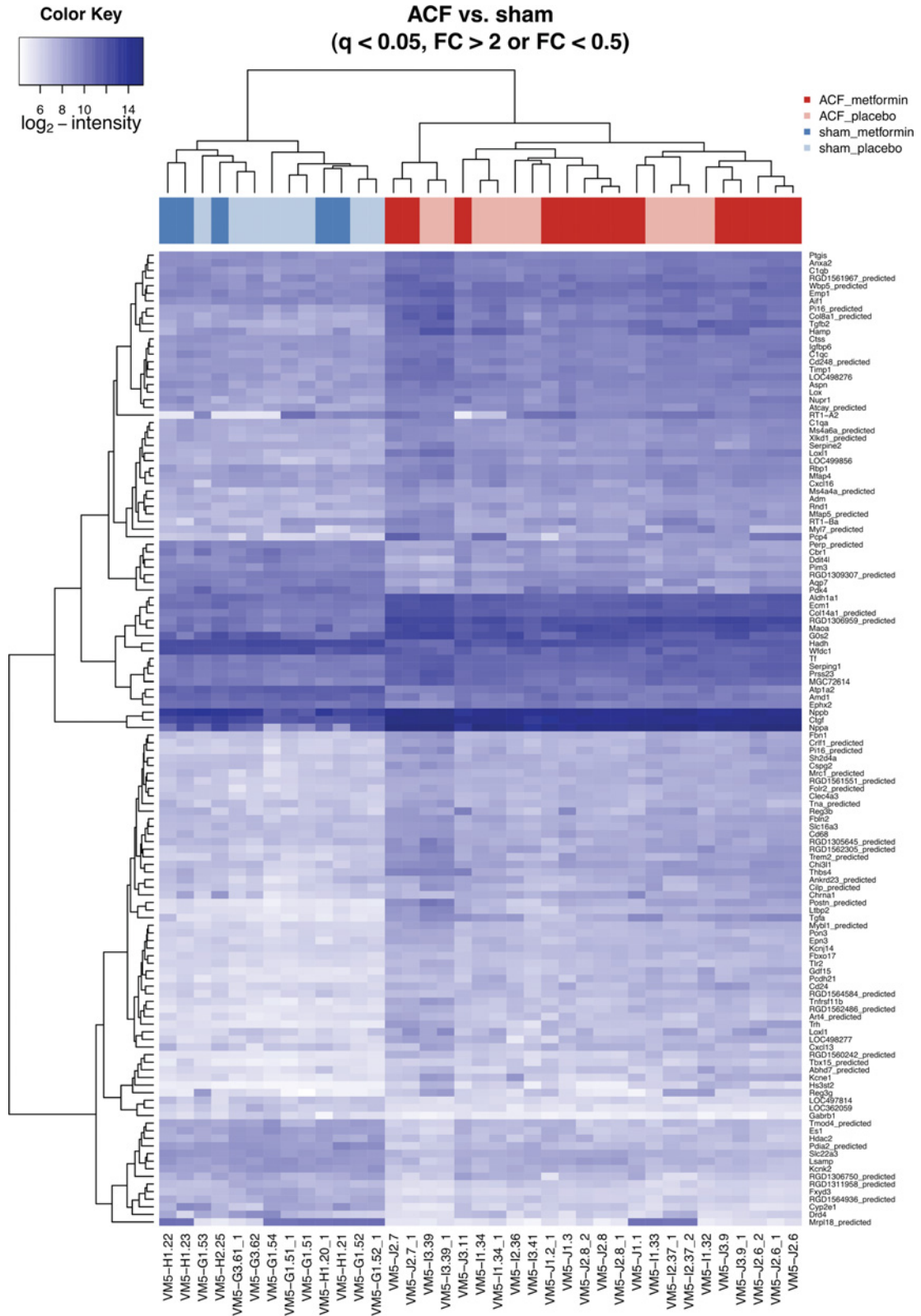
Figure S3   Transcription profiles of animals with ACF differ significantly from the profiles of sham-operated animals, irrespective of MET treatment

A heatmap of all significantly differentially expressed transcripts between either treated or untreated sham and ACF animals (SH+PL compared with ACF+PL and SH+MET compared with ACF+MET) is shown. All transcripts with the Storey's q-value <0.05 and 2-fold or greater change in intensity in at least one of the two contrasts are presented. A darker colour reflects a greater quantity of the transcript. Gene symbols are given next to the transcript they refer to.

Table S1   Results of GSEA on KEGG pathways significantly down-regulated for ACF+PL compared with SH+PL

Metabolic changes in animals with ACF: all significantly down-regulated KEGG pathways between placebo-treated sham-operated animals (SH+PL) and animals with the ACF (ACF+PL), with a false discovery rate <0.05.

Pathway ID	Pathway name	False discovery rate of pathway down-regulation
rno00071	Fatty acid metabolism	<0.0001
rno00280	Valine, leucine and isoleucine degradation	<0.001
rno00062	Fatty acid elongation in mitochondria	0.002
rno00640	Propanoate metabolism	0.04

by weighted linear regression (weighing factor $1/x^2$): the analyte peak area was plotted compared with the analyte concentration. In case of a sample with a concentration above the upper limit of quantification, dilution with a blank serum and re-analysis was applied.

REFERENCES

1 Garcia, R. and Diebold, S. (1990) Simple, rapid, and effective method of producing aortocaval shunts in the rat. Cardiovasc. Res. **24**, 430–432

2 Brower, G. L. and Janicki, J. S. (2001) Contribution of ventricular remodeling to pathogenesis of heart failure in rats. Am. J. Physiol. Heart Circ. Physiol. **280**, H674–H683

3 Ruzicka, M., Yuan, B., Harmsen, E. and Leenen, F. H. (1993) The renin–angiotensin system and volume overload-induced cardiac hypertrophy in rats. Effects of angiotensin converting enzyme inhibitor versus angiotensin II receptor blocker. Circulation **87**, 921–930

4 Cantor, E. J., Babick, A. P., Vasanji, Z., Dhalla, N. S. and Netticadan, T. (2005) A comparative serial echocardiographic analysis of cardiac structure and function in rats subjected to pressure or volume overload. J. Mol. Cell. Cardiol. **38**, 777–786

4a Gundersen, H. J. and Jensen, E. B. (1987) The efficiency of systematic sampling in stereology and its prediction. J. Microsc. **147**, 229–263

5 Nouette-Gaulain, K., Malgat, M., Rocher, C., Savineau, J. P., Marthan, R., Mazat, J. P. and Sztark, F. (2005) Time course of differential mitochondrial energy metabolism adaptation to chronic hypoxia in right and left ventricles. Cardiovasc. Res. **66**, 132–140

6 Dunning, M. J., Smith, M. L., Ritchie, M. E. and Tavare, S. (2007) beadarray: R classes and methods for Illumina bead-based data. Bioinformatics **23**, 2183–2184

7 Gentleman, R. C., Carey, V. J., Bates, D. M., Bolstad, B., Dettling, M., Dudoit, S., Ellis, B., Gautier, L., Ge, Y., Gentry, J. et al. (2004) Bioconductor: open software development for computational biology and bioinformatics. Genome Biol. **5**, R80

8 Strnad, H., Lacina, L., Kolar, M., Cada, Z., Vlcek, C., Dvorankova, B., Betka, J., Plzak, J., Chovanec, M., Sachova, J. et al. (2010) Head and neck squamous cancer stromal fibroblasts produce growth factors influencing phenotype of normal human keratinocytes. Histochem. Cell. Biol. **133**, 201–211

9 Smyth, G. K. (2005) Limma: linear models for microarray data. In Bioinformatics and Computational Biology Solutions using R and Bioconductor (Gentleman, V., and, Carey, S., Carey, Dudoid, S., Irizarry, R. and Huber, W., eds.), pp. 397–420, Springer, New York

10 Storey, J. D. (2003) The positive false discovery rate: a Bayesian interpretation and the q-value. Ann. Stat. **31**, 2013–2035

11 Kanehisa, M. and Goto, S. (2000) KEGG: kyoto encyclopedia of genes and genomes. Nucleic Acids Res. **28**, 27–30

12 Tian, L., Greenberg, S. A., Kong, S. W., Altschuler, J., Kohane, I. S. and Park, P. J. (2005) Discovering statistically significant pathways in expression profiling studies. Proc. Natl. Acad. Sci. U.S.A. **102**, 13544–13549

13 Benjamini, Y. and Hochberg, Y. (1995) Controlling the false discovery rate: a practical and powerful approach to multiple testing. J. R. Stat. Soc. Ser. B Stat. Methodol. **57**, 289–300

14 Argaud, D., Roth, H., Wiernsperger, N. and Leverve, X. M. (1993) Metformin decreases gluconeogenesis by enhancing the pyruvate kinase flux in isolated rat hepatocytes. Eur. J. Biochem. **213**, 1341–1348

15 Kus, V., Prazak, T., Brauner, P., Hensler, M., Kuda, O., Flachs, P., Janovska, P., Medrikova, D., Rossmeisl, M., Jilkova, Z. et al. (2008) Induction of muscle thermogenesis by high-fat diet in mice: association with obesity-resistance. Am. J. Physiol. Endocrinol. Metab. **295**, E356–E367

16 Mracek, T., Pecinova, A., Vrbacky, M., Drahota, Z. and Houstek, J. (2009) High efficiency of ROS production by glycerophosphate dehydrogenase in mammalian mitochondria. Arch. Biochem. Biophys. **481**, 30–36

17 Drahota, Z., Milerova, M., Stieglerova, A., Houstek, J. and Ostadal, B. (2004) Developmental changes of cytochrome c oxidase and citrate synthase in rat heart homogenate. Physiol. Res. **53**, 119–122

18 Pecina, P., Capkova, M., Chowdhury, S. K., Drahota, Z., Dubot, A., Vojtiskova, A., Hansikova, H., Houst'kova, H., Zeman, J., Godinot, C. and Houstek, J. (2003) Functional alteration of cytochrome c oxidase by SURF1 mutations in Leigh syndrome. Biochim. Biophys. Acta **1639**, 53–63

19 Cahova, M., Vavrinkova, H., Meschisvilli, E., Markova, I. and Kazdova, L. (2004) The impaired response of non-obese hereditary hypertriglyceridemic rats to glucose load is associated with low glucose storage in energy reserves. Exp. Clin. Endocrinol. Diabetes **112**, 549–555

20 Cahova, M., Vavrinkova, H., Tutterova, M., Meschisvilli, E. and Kazdova, L. (2003) Captopril enhanced insulin-stimulated glycogen synthesis in skeletal muscle but not fatty acid synthesis in adipose tissue of hereditary hypertriglyceridemic rats. Metab. Clin. Exp. **52**, 1406–1412

21 Kraegen, E. W., Jenkins, A. B., Storlien, L. H. and Chisholm, D. J. (1990) Tracer studies of in $vivo$ insulin action and glucose metabolism in individual peripheral tissues. Horm. Metab. Res. Suppl. **24**, 41–48

22 Russell, III, R. R., Bergeron, R., Shulman, G. I. and Young, L. H. (1999) Translocation of myocardial GLUT-4 and increased glucose uptake through activation of AMPK by AICAR. Am. J. Physiol. **277**, H643–H649

23 Sugimoto, K., Kazdova, L., Qi, N. R., Hyakukoku, M., Kren, V., Simakova, M., Zidek, V., Kurtz, T. W. and Pravenec, M. (2008) Telmisartan increases fatty acid oxidation in skeletal muscle through a peroxisome proliferator-activated receptor-gamma dependent pathway. J. Hypertens. **26**, 1209–1215